

Supplementary Materials for

RAS engages AGO2 to enhance cellular transformation

Sunita Shankar,^{1,2} Sethuramasundaram Pitchiaya,^{1,2,3} Rohit Malik,^{1,2} Vishal Kothari,^{1,2} Yasuyuki Hosono,^{1,2} Anastasia Yocum,^{1,2} Harika Gundlapalli,^{1,2} Yasmine White,⁴ Ari Firestone,⁴ Xuhong Cao,^{1,5} Saravana M. Dhanasekaran,^{1,2} Jeanne A. Stuckey,^{6,7} Gideon Bollag,⁸ Kevin Shannon,⁴ Nils G. Walter,³ Chandan Kumar-Sinha,^{1,2} Arul M. Chinnaiyan^{1,2,5,9,10*}

¹Michigan Center for Translational Pathology, University of Michigan, Ann Arbor, MI 48109, USA.

²Department of Pathology, University of Michigan, Ann Arbor, MI 48109, USA.

³Single Molecule Analysis Group, Department of Chemistry, University of Michigan, Ann Arbor, MI 48109, USA.

⁴Department of Pediatrics and Helen Diller Family Comprehensive Cancer Center, University of California, San Francisco, San Francisco, CA 94158, USA.

⁵Howard Hughes Medical Institute, University of Michigan, Ann Arbor, MI 48109, USA.

⁶Life Science Institute, University of Michigan, Ann Arbor, Michigan 48109, USA

⁷Department of Biological Chemistry, University of Michigan, Ann Arbor, Michigan 48109, USA.

⁸Plexxikon Inc., Berkeley, CA 94710, USA.

⁹Comprehensive Cancer Center, University of Michigan, Ann Arbor, MI 48109, USA.

¹⁰Department of Urology, University of Michigan, Ann Arbor, MI 48109, USA.

*Corresponding author:

Arul M. Chinnaiyan, M.D., Ph.D.
Investigator, Howard Hughes Medical Institute
American Cancer Society Professor
S. P. Hicks Endowed Professor of Pathology
Comprehensive Cancer Center
University of Michigan Medical School
1400 E. Medical Center Dr. 5316 CCGC
Ann Arbor, MI 48109-0602
Email: arul@umich.edu

Key words: cancer, KRAS, EIF2C2, Argonaute 2, RNA silencing

This PDF contains
Supplemental Figures S1-S7
Supplemental Tables 1-4

Figure S1

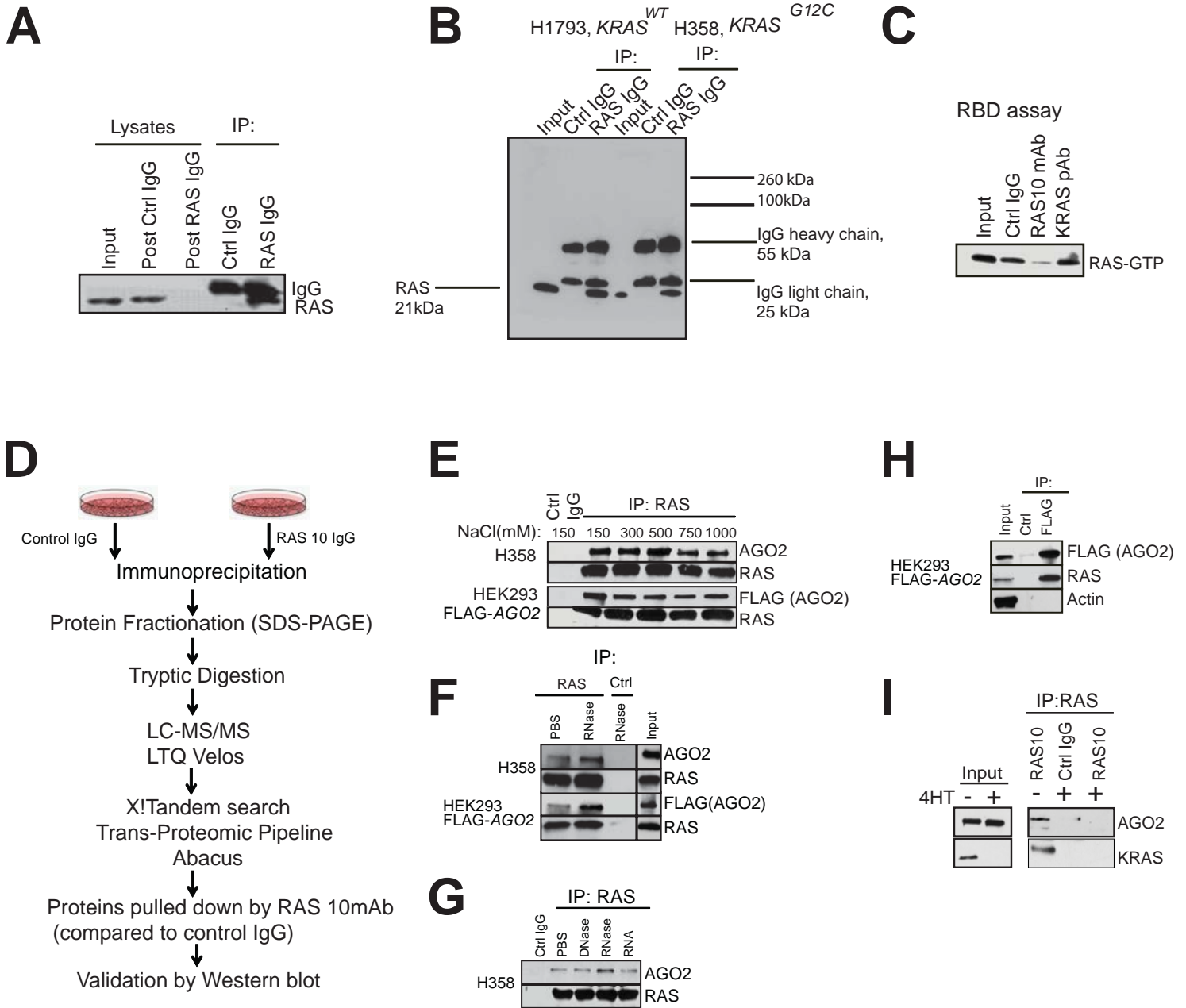
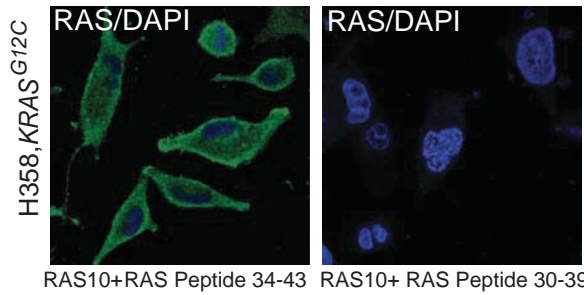


Figure S1. Related to Figure 1. Characterization of RAS10 mAb, used for mass spectrometric identification of RAS-AGO2 interaction, validated by immunoblot analysis in the presence of RNase. (A) Efficiency of the RAS10 mAb in pulling down RAS as seen by immunoblot analysis of RAS immunoprecipitates. The RAS10 mAb was used for both immunoprecipitation (IP) and immunoblot (IB) analysis. (B) Scan of the entire immunoblot using the RAS10 mAb demonstrating the specificity of detection using total cell lysates or immunoprecipitates. Both the IP and immunoblotting were performed using the RAS10 mAb. (C) Immunoblot analysis of RAS bound to RAS binding domain of RAF (RBD) in the presence of different RAS antibodies. RBD agarose beads were added to H358 cell lysates in the presence of RAS10 monoclonal or KRAS polyclonal (KRAS sc-521) antibody. Reduced interaction between RAS-GTP and RBD in the presence of RAS10 antibody indicates that the antibody binds the RAS Switch I domain and interferes with the RAS-RAF interaction. KRAS sc-521 polyclonal antibody, which binds the C-terminal region of KRAS was used as control. RAS10 mAb was used for IB analysis. (D) Schematic of the methodology used for RAS Co-IP MS. Proteins pulled down by the corresponding isotypic control IgG in each cell line were considered as non-specific hits and were excluded from the data obtained from RAS IP. (E) IP of RAS in H358 and HEK293 FLAG-AGO2 expressing cells under increasing concentrations of salt followed by immunoblot analysis. Immunoblot analysis of RAS10 Ab immunoprecipitates from H358 lung cancer (endogenous) and FLAG-AGO2 overexpressing HEK293 cell lysates treated with RNase (F) and DNase (G). RAS10 mAb was used for both IP and IB. RAS10 mAb was used for both IP and IB. (H) FLAG tagged AGO2 expressed in HEK293 immunoprecipitates RAS. Actin was used as control. (I) Co-IP analysis in RASless MEFs demonstrates specificity of RAS-AGO2 interaction. Genetically engineered mouse embryonic fibroblasts expressing KRAS were treated with 4-hydroxytamoxifen prior to co-IP using RAS10 antibody. Immunoblot analysis shows tamoxifen treated RASless MEFs abrogate KRAS expression and fail to immunoprecipitate AGO2.

Figure S2

A



B

Organelle	Region	Blue / Green	Blue / Red	Green / Red
Mitochondria	I	0.34	0.15	0.06
	II	0.17	0.45	0.20
	III	0.04	0.04	0.19
Golgi	I	0.36	0.20	0.17
	II	0.20	0.30	0.35
	III	0.37	0.27	0.17
Endosomes	I	0.31	0.30	0.17
	II	0.30	0.47	0.18
	III	0.14	0.23	0.11
ER	I	0.62	0.53	0.62
	II	0.21	0.35	0.15
	III	0.53	0.58	0.58

C

MIA PaCa-2, KRAS^{G12C}

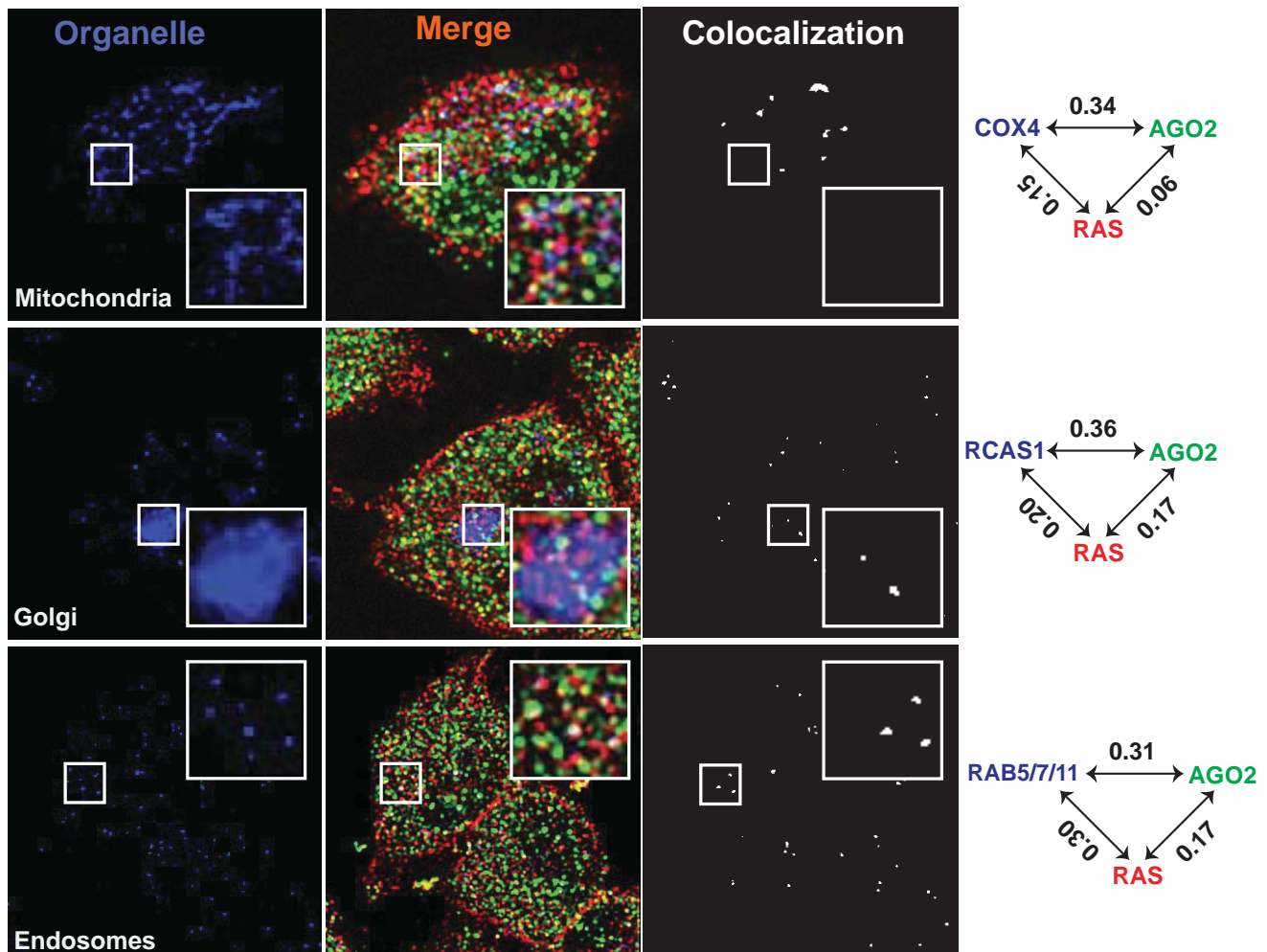
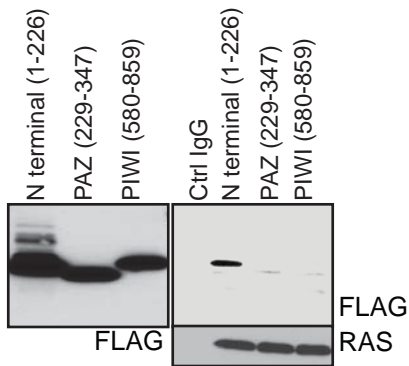
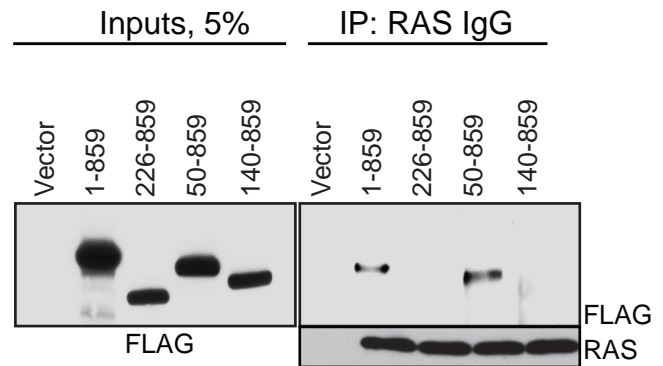


Figure S2. Related to Figure 2. Specificity of RAS10 mAb and co-localization of RAS and AGO2 in the endoplasmic reticulum (A) Specificity of the RAS10 mAb is demonstrated by pre-incubating the antibody with switch I domain specific (30-39aa) or non-specific (34-43aa) RAS peptides, prior to immunofluorescence analysis. As seen, both the membrane-bound and intracellular staining was abrogated upon pre-incubation of the RAS10 Ab with RAS peptide spanning the RAS10 Ab epitope in the Switch I effector domain (aa 30-39) but not by a RAS peptide spanning the neighboring aa 34-43. (B) Pairwise Manders overlap coefficients within 3 randomly selected regions for each organelle. Extent of colocalization within Region I is indicated in Figure 2D. Maximum overlap (marked in yellow) between RAS and AGO2 signals (green/red) is observed in the ER where both proteins are abundantly present. (C) Representative images of immunofluorescence analysis of AGO2 (green), RAS (red) and different membrane bound organelles (blue) in MiaPaCa-2 cells. White spots indicate colocalization signals for RAS/AGO2/organelle in each panel. Pairwise Manders overlap coefficients are shown on the right. The inset shows a magnified 6.7 μm x 6.7 μm view of the areas marked. Scale bar, 5 μm .

A Inputs,5% IP:RAS



B



C

```

AGO3 --MEIGSAGPAG-----AQPLLMVPRRPGYGTMGKPIKLLANCFQVEIPKIDVLYEVD 52
AGO4 ----MEALGPGP-----PASLFQPPRRPGLGTVGKPIRLLANHFQVQIPKIDVYHYDVD 50
AGO1 --MEAGPSGAAAGAYLPPLQQVFQAPRRPGIGTVGKPIKLLANYFEVDIPKIDVYHYEVD 58
AGO2 MYSGAGPALAPPAPPPPIQGYAFKPPRPDFGTSGRTIKLQANFFEMDIPKIDIYHYELD 60
      . . . . . : * * * . * * * : * * * * * : * * * * * * * * * * * * * * * *
                                          59

AGO3 IKPDKCPRRVNREVVDMSVQHFKVTIFGDRRPVYDGKRSLYTANPLPVATTGVLDLDTLP 112
AGO4 IKPEKRPRRVNREVVDTMVRHFQMIFGDRQPGYDGKRNMYTAHPLPIGRDRVDM EVTLP 110
AGO1 IKPDKCPRRVNREVVEYMQVHFKPQIFGDRKPVYDGKKNIIYTVTALPIGNERVDFEVTIP 118
AGO2 IKPEKCPRRVNREIVEHMQVHFKTQIFGDRKPVFDGRKNLYTAMPLPIGRDKVELEVTLP 120
      * * * * * * * * * * * * * * * * * * * * * * * * * * * * * * * * * * * * * * * * *
      74 77 84 94 97 98 104 112 114

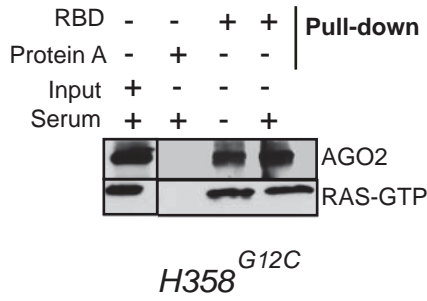
AGO3 GEGGKDRPFKVSIKFVSRVSWHLLHEVLTGRTLPEPLELDKPISTNPVHAVDVVLRHLPS 172
AGO4 GEG-KDQTFKVSQWVSVVSLQLLLEALAG-----HLN-EVPDDSVQALDVITRHLPS 161
AGO1 GEG-KDRIFKVSIKWLAIIVSWRMLHEALVSG-----QIPVPLESVQALDVAMRHLAS 169
AGO2 GEG-KDRIFKVSIKWVCVSLQALHDALSGR-----LPSVPFETIQALDVVMRHLPS 171
      * * * * * * * * * * * * * * * * * * * * * * * * * * * * * * * * * * * * * * * * *
      137

WEDGE DOMAIN:50-139aa
  
```

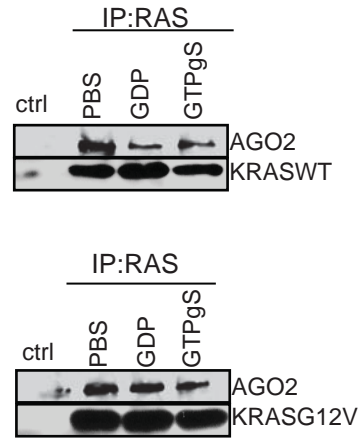
Figure S3. Related to Figure 3. The N-terminal domain of AGO2 is necessary and sufficient to bind RAS. (A) Expression (left panel) and RAS IP interaction analysis (right panel) of FLAG tagged N-terminal, PAZ, or PIWI domains of *AGO2* in HEK293 cells. Immunoblot analysis shows that (1-226aa) N terminal domain is sufficient for RAS interaction using RAS10mAb. (B) Expression (left panel) and RAS IP analysis (right panel) of various indicated *AGO2* N terminal deletion constructs in HEK293 cells. Immunoblot analysis indicates that 50-139 aa in the *AGO2* N terminal domain is essential for RAS binding. Both RAS IP and IB were performed using RAS10 mAb. (C) ClustalW alignment of the Argonaute family proteins spanning the “wedge domain” (50-139 aa, marked in grey). Residues marked in yellow were identified as unique to *AGO2* and were mutagenized to alanine for binding analysis. The numbers below indicate the amino acid position. *AGO2*^{K98} (marked in green) shared with *AGO1* was also changed to alanine to be used as control. *AGO2* residues K112 and E114, marked in red were critical for RAS interaction.

Figure S4

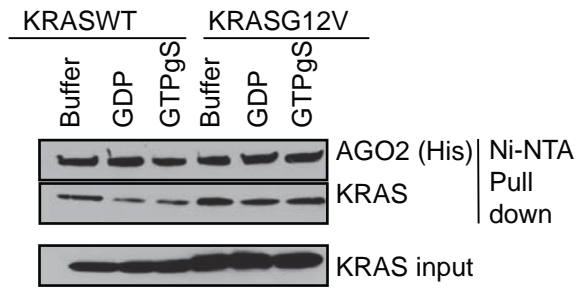
A



B



C



D

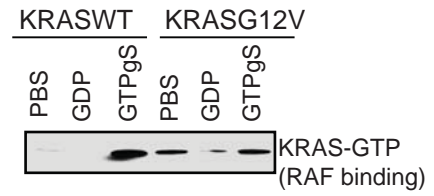
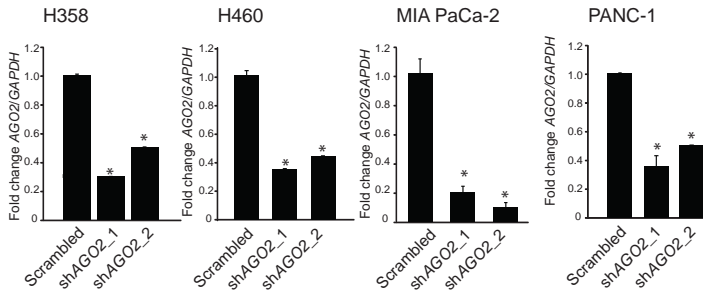


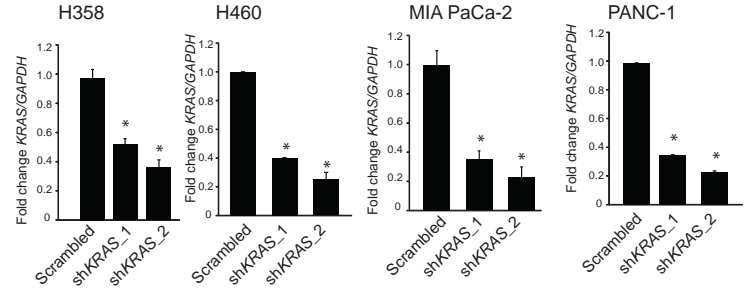
Figure S4. Related to Figure 4. RAS binds AGO2 through its Switch II domain and agnostic to nucleotide bound to RAS (A) RBD pull down assay using 1mg of lysates from H358 cells followed by immunoblot analysis for RAS (RAS10) and AGO2 (AGO2, 11A9). (B) GDP or GTP γ S loading of recombinant KRASWT (top panel) and KRASG12V (bottom panel) proteins prior to RAS-AGO2 *in vitro* co-IP analysis using RAS10 Ab. (C) *In vitro* HIS-AGO2 pull down assay after GDP or GTP γ S loading of recombinant KRASWT and KRASG12V proteins. (D) RBD pull down assay using recombinant KRASWT and KRASG12V proteins loaded with GDP or GTP γ S to demonstrate efficiency and specificity of nucleotide loading. Immunoblot analysis for RAS and AGO2 was performed using the RAS10 and AGO2, 11A9 antibodies.

Figure S5

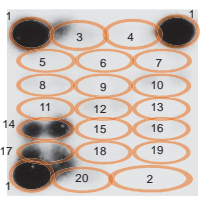
A



B

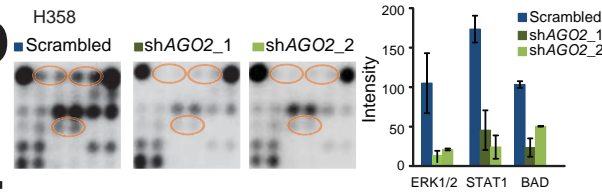


C

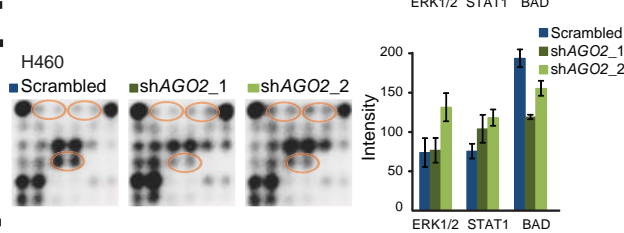


Number	Target	Target Site	Modification
1	Positive Control	N/A	N/A
2	Negative Control	N/A	N/A
3	Erk1/2	Thr202/Tyr204	Phosphorylation
4	Stat1	Tyr701	Phosphorylation
5	Stat3	Tyr705	Phosphorylation
6	Akt	Thr308	Phosphorylation
7	Akt	Ser473	Phosphorylation
8	AMPKa	Thr172	Phosphorylation
9	S6 Ribosomal	Ser235/236	Phosphorylation
10	mTOR	Ser2448	Phosphorylation
11	HSP27	Ser78	Phosphorylation
12	Bad	Ser112	Phosphorylation
13	p70 S6 Kinase	Thr389	Phosphorylation
14	PRAS40	Thr246	Phosphorylation
15	p53	Ser15	Phosphorylation
16	p38	Thr180/Tyr182	Phosphorylation
17	SAPK/JNK	Thr183/Tyr185	Phosphorylation
18	PARP	Asp214	Cleavage
19	Caspase-3	Asp175	Cleavage
20	GSK-3β	Ser9	Phosphorylation

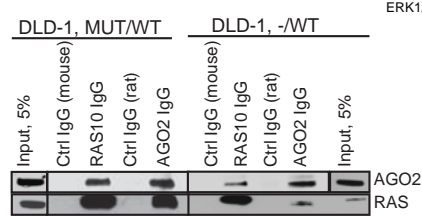
D



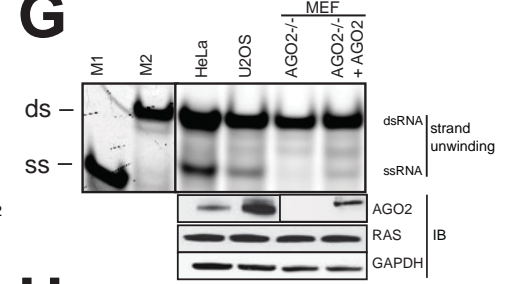
E



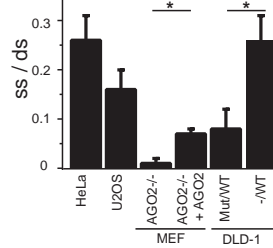
F



G



H



I

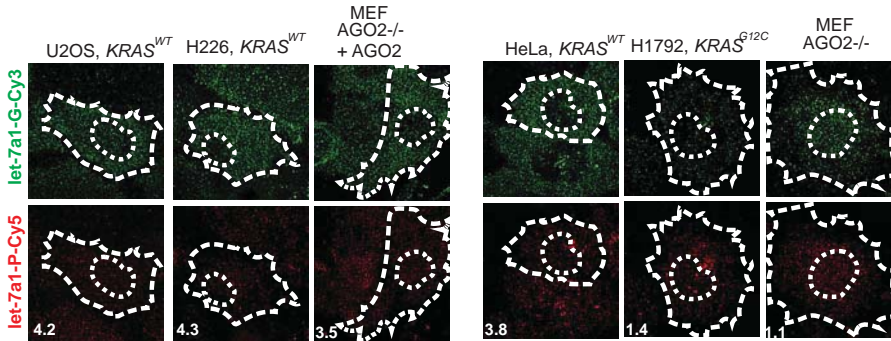


Figure S5. Related to Figure 5. Effects of AGO2 knockdown on RAS signaling and inhibition of AGO2 function in mutant KRAS expressing human cancer cell lines. qRT-PCR of *AGO2* and *KRAS* transcripts demonstrating the efficiency of *AGO2* (A) and *KRAS* (B) knockdown in the indicated lung and pancreatic cancer cells. Representative assessments are shown. Error bars show standard error of mean and asterisks indicate P values less than 0.05 in each condition. (C) Top, representative image of an intracellular signaling array (probed with lysates from NIH3T3 expressing empty vector) used to show the position of target spots of various signaling molecules indicated in the table shown below. Intracellular signaling arrays probed with lysates from *KRAS*-dependent H358 (D) and *KRAS*-independent H460 (E) lung cancer cells, following knockdown of *AGO2* by two independent shRNAs. Quantification of signal intensities of indicated proteins normalized against control spots, right panel. Parts of these images have been used in Figs. 4d and 4f. (F) Co-IP analysis using RAS and AGO2 antibodies show RAS-AGO2 interaction in the DLD-1 isogenic cells expressing *KRAS*^{G12C} (MUT/WT) or *KRAS*^{WT} (-/WT). (G) Upper panel shows representative images of native acrylamide gel electrophoretic analysis of *let-7* microRNA unwinding in the indicated cellular extracts. M1 and M2 represent double (ds) and single stranded (ss) markers respectively. (n = 2, *p < 0.05) and shared with Figure 7B in the same electrophoretic run. Lower panel shows immunoblot analysis of the indicated proteins. (H) Quantitation of the gel electrophoretic analysis of *let-7* unwinding within different protein extracts. (I) Representative Images of the guide strand (green) and passenger strand (red) of *let-7* microRNA in the indicated cell lines, 30 mins post injection. Numbers in the boxes indicate Guide: passenger strand ratio. Scale bar, 10 μ m.

Figure S6

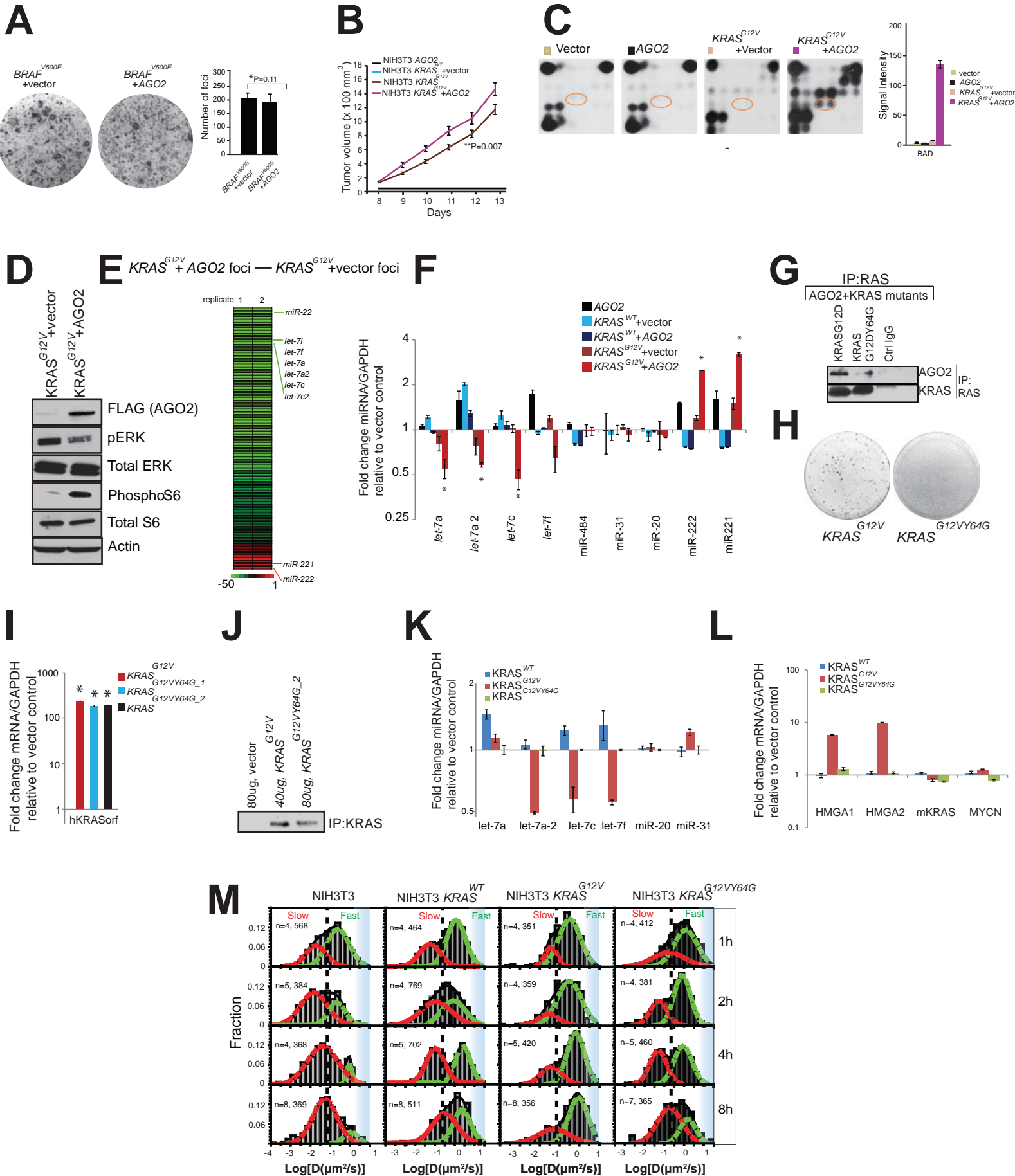


Figure S6. Related to Figure 6. Oncogenic KRAS interacts with AGO2 to inhibit RISC function, a requisite for foci formation in NIH3T3 cells. (A) Representative images of foci formation assays using NIH3T3 cells co-transfected with *BRAF*^{V600E} ± *AGO2*. Quantitation of foci from two independent experiments (right). Error bars show standard error of mean of 2 replicates and P value was calculated using two sided t-test. (B) *In vivo* growth of NIH3T3 cells stably overexpressing *AGO2*, *KRAS*^{WT}, *KRAS*^{G12V}+vector, or *KRAS*^{G12V}+*AGO2* in nude mice. For each group (n=8), 500,000 cells were injected and average tumor volume (in mm³) was plotted on y-axis and days after injection on the x-axis. (C) Left, Images of the intracellular signaling arrays probed with lysates from NIH3T3 cells stably expressing vector, *AGO2*, or *KRAS*^{G12V}+/-*AGO2*. The colored circles mark duplicate spots corresponding to p-BAD, left panel. Right, Quantification of signal intensities of p-BAD normalized to control spots, right panel. Parts of these images have been used in Fig. 5b. (D) Immunoblot analysis of signaling molecules in lysates expressing *KRAS*^{G12V}+/- *AGO2* described above. (E) High throughput sequencing analysis of mature microRNA expression levels in RNA obtained from NIH3T3 foci upon co-transfection of *KRAS*^{G12V}+*AGO2* compared to *KRAS*^{G12V}+vector. Heat map indicates differences in normalized read counts for individual microRNAs in the two samples performed in duplicate. The green and red colors denote downregulated (214/781) and upregulated (29/781) mature microRNAs, respectively. The colored scale below shows significant differences in normalized read counts of mature microRNA expression. (F) qRT-PCR analysis of *let-7* and the *miR-221/miR-222* family of microRNAs from NIH3T3 cells expressing *AGO2* or *KRAS* constructs (*KRAS*^{WT} or *KRAS*^{G12V}) alongwith vector or *AGO2*, obtained from the foci assay. U6 RNA was used as a control to normalize the data and vector transfected cells were used as reference. Error bars show standard error of the mean of 4 replicates and asterisks indicate significant log2 fold changes (two sided t-test, P-value less than 0.05) between the indicated conditions compared to vector control. (G) *In vitro* co-IP analysis of *KRAS*-*AGO2* interaction with recombinant *KRAS*G12D and *KRAS*G12DY64G proteins, using RAS10 Ab. (H) Lack of foci formation of an independent construct encoding *KRAS*^{G12VY64G}. (I) qRT-PCR analysis of human *KRAS* orf transcripts stably expressed in NIH3T3 cells, by plasmids encoding *KRAS*^{G12V} or two independent clones of *KRAS*^{G12VY64G}. (J) Immunoprecipitation (IP:KRAS antibody, sc-521) followed by immunoblot analysis (IB: RAS10) of polyclonal populations of NIH3T3 cells stably expressing an independent construct encoding *KRAS*^{G12VY64G}. The amount of total lysate used for IP-IB analysis is indicated in the blot. qPCR analysis of *let-7* family microRNAs (K) and *let-7* microRNA targets (L) from NIH3T3 cells stably expressing *KRAS*^{WT}, *KRAS*^{G12V} or *KRAS*^{G12VY64G} constructs. U6 RNA and GAPDH mRNA were used as controls to normalize the microRNA and mRNA data respectively and vector transfected cells were used as reference. Target genes *HMGAI/2*, *KRAS* and *MYCN* are known to be regulated by *let-7* microRNA. Error bars show standard error of the mean of 4 replicates and asterisks indicate significant log2 fold changes (two sided t-test, P-value less than 0.05) between the indicated conditions compared to vector control. (M) Distribution of *let-7a-1*-Cy5 diffusion coefficients at different time points following microinjection in parental NIH3T3, NIH3T3^{WT} NIH3T3-*KRAS*^{G12V} and NIH3T3-*KRAS*^{G12V,Y64G} cells, as described earlier (Pitchiaya et al., 2012). The fast (green) and slow (red) diffusing particles (demarcated by the dotted lines to guide the eye) were defined based on segregation of the two Gaussian distributions 2h after microinjection. Blue shaded region represents the diffusion coefficients lost due to limited time resolution of tracking. Number of particles analyzed is mentioned within each histogram.

Figure S7

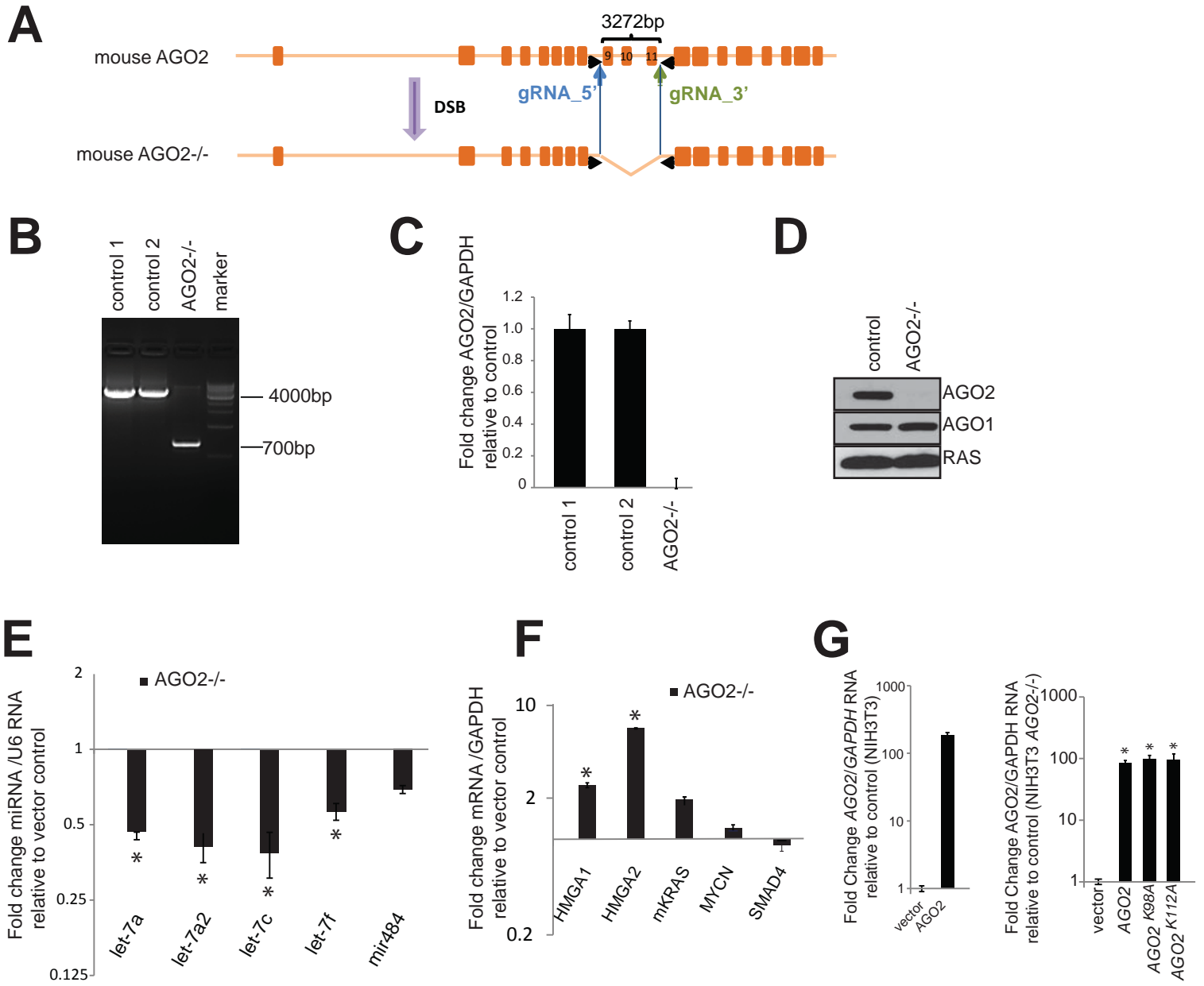


Figure S7. Related to Figure 7. Generation and characterization of NIH3T3 *AGO2*^{-/-} cells.

(A) Schematic showing the use of the CRISPR/Cas9 methodology to knockout *AGO2* in NIH3T3 cells. Validation of *AGO2* knockout was performed using genomic PCR (B), RT-qPCR (C), and immunoblot analysis (D). qPCR analysis of *let-7* family microRNAs (E) and their target genes (F) in NIH3T3 *AGO2*^{-/-} cells. Both the microRNA and transcript levels were compared to NIH3T3 cells treated with vector with no guide RNA. Error bars show standard error of the mean of 4 technical replicates and asterisks indicate significant log₂ fold changes (two sided t-test, P-value less than 0.05) between the indicated conditions. (G) qPCR analysis of *AGO2* transcripts in NIH3T3 (left) and NIH3T3 *AGO2*^{-/-} (right) cells two days after transfection for foci formation assay, demonstrating similar levels of expression of *AGO2* constructs. Error bars show standard error of the mean of 3 technical replicates and asterisks indicate significant log₁₀ fold changes (two sided t-test, P-value less than 0.005) in *AGO2* expression over that of the vector control.

Table S1. Related to Figure 1

Number	Cell Line	Source	Tissue	Type	<i>KRAS</i> or <i>AGO2</i> status	RAS co-IP Mass Spec	RAS co-IP Western
1	A549	Human	Lung	Cancer	<i>KRAS</i> G12S	X	ND
2	H2009	Human	Lung	Cancer	<i>KRAS</i> G12A	ND	X
3	H358	Human	Lung	Cancer	<i>KRAS</i> G12C	X	X
4	H441	Human	Lung	Cancer	<i>KRAS</i> G12V	X	ND
5	H460	Human	Lung	Cancer	<i>KRAS</i> Q61H	ND	X
6	H727	Human	Lung	Cancer	<i>KRAS</i> G12V	X	X
7	BXPC3	Human	Pancreas	Cancer	<i>KRAS</i> WT	X	X
8	CAPAN-1	Human	Pancreas	Cancer	<i>KRAS</i> G12V	X	ND
9	MIA PaCa-2	Human	Pancreas	Cancer	<i>KRAS</i> G12C	X	X
10	PANC-1	Human	Pancreas	Cancer	<i>KRAS</i> G12D	X	ND
11	PDX 1319	Human	Pancreas	Cancer	<i>KRAS</i> G12D	X	ND
12	PL-45	Human	Pancreas	Cancer	<i>KRAS</i> G12D	X	ND
13	HPNE	Human	Pancreas	Benign	<i>KRAS</i> WT	ND	X
14	DLD-1 (MUT/WT)	Human	Colorectal	Cancer	G13D	ND	X
15	DLD-1 (-/WT)	Human	Colorectal	Benign	WT	ND	X
16	H1792	Human	Lung	Cancer	G12C	ND	ND
17	H226	Human	Lung	Cancer	WT	ND	ND
18	HEK293FT	Human	Embryonic kidney	Benign	for transient overexpression as indicated	ND	X
19	MEF _{parental}	Mouse	Embryonic fibroblast	Benign		ND	X
20	<i>AGO2</i> MEF ^{-/-}	Mouse	Embryonic fibroblast	Benign	<i>AGO2</i> knockout	ND	X
21	<i>AGO2</i> MEF ^{-/-} + <i>AGO2</i>	Mouse	Embryonic fibroblast	Benign	<i>AGO2</i> knockout overexpressing	ND	X

Supplemental Table S1. Cell lines used in the study. Cell lines used in this study for RAS co-IP MS and/or RAS co-IP Western blot analysis and other assays, with their associated *KRAS* mutation status. NIH3T3 stable lines were generated using plasmids encoding *KRAS*^{WT} or *KRAS*^{G12V}. HEK293 cells were used for transfection for assays in the transient mode. PDX 1319 is a pancreatic cancer derived xenograft cell line.

Table S2. Related to Figure 1

Protein ID	Protein	Lung				Pancreas							Mouse fibroblast		Cumulative spectral counts	Number of cancer cell lines
		A549	H358	H441	H727	BXPC3	Capan-1	MIA PaCa-2	PANC-1	PL45	PDX 1319	NIH3T3 KRAS ^{G12V}	NIH3T3 KRAS ^{WT}			
NP_004976/ NP_002515/ NP_005334	KRAS/NRAS/HRAS	20	44	52	112	75	33	23	36	16	33	98	34	556	12	
NP_036286	EIF2C2 (AGO2)	16	45	9	18	38	1	14	12	4	9	48	39	237	12	
NP_004090	STOM	0	40	16	56	21	3	0	13	3	2	5	6	165	10	
NP_001138303	PHB2	0	3	23	0	5	48	0	15	48	4	7	9	162	10	
NP_258260	FCHSD1	26	20	0	0	0	13	0	11	13	0	8	11	76	7	
NP_057018	NOP58	10	19	31	0	3	4	4	2	4	6	0	0	73	9	
NP_001028886	NOP2	10	13	15	0	2	9	0	0	9	2	0	0	50	7	
NP_542193	BR13BP	0	3	3	20	0	3	3	2	3	3	0	0	40	8	
NP_005605	RHEB	10	3	9	0	5	0	0	0	0	7	11	0	35	6	
NP_055315	HTATSF1	9	29	0	0	0	2	0	2	2	0	0	0	35	5	
NP_036473	GTPBP4	6	2	13	0	0	0	8	0	0	1	0	0	24	5	
NP_055118	PES1	5	5	9	0	0	0	5	0	0	3	0	0	22	5	
NP_078938	NAT10	6	9	1	0	0	2	4	1	2	1	0	0	20	8	
NP_001092688	RAD51AP2	5	4	0	0	0	6	0	4	6	0	0	0	20	5	

Supplemental Table S2. Summary of shared peptide hits in RAS coIP mass spectrometry in cancer cell lines. Spectral counts of peptides detected in at least 5 of 10 cancer cell lines tested by tandem mass spectrometry of RAS co-immunoprecipitation.

Table S3. Antibodies used for immunoprecipitation and immunoblotting

#	Antibody	Vendor	Catalog Number	Experiments	Validation method/s	Specificity
1	Anti-Ras Clone 10	Millipore	05-516	IP, IB, IF	recombinant protein detection, peptide competition	human and mouse
2	K-Ras-2B Antibody (C-19)	Santa Cruz	sc-521	IP, IB, IF	recombinant protein detection, KRAS siRNA	only human
3	K-Ras monoclonal Ab	Santa Cruz	sc-30	IB	recombinant protein detection	human and mouse
4	RAS Y13-259 rat monoclonal	Abcam	ab79973	IP	recombinant protein detection	human
5	AGO2 rabbit pAb	Millipore	07-590	IP, IB	recombinant protein detection	human
6	AGO2 mouse mAb, clone 2E12-1C9	Sigma	WH0027161M1	IP, IB, IF	recombinant protein detection	human and mouse
7	AGO2, 11A9	Sigma	SAB4200085	IP, IB, IF	recombinant protein detection	only human
8	Anti-Flag	Sigma	F1804	IB, IP	FLAG-AGO2 detection in HEK 293 cells	NA
9	phospho-Akt S-473	Cell Signaling	4060S	IB	ND	human and mouse
10	phospho-ERK	Cell Signaling	4370	IB	ND	human and mouse
11	SAM68	Santa Cruz	sc-733	IB	ND	human
12	GAPDH-HRP	Cell Signaling	3683	IB	ND	human and mouse
13	Actin	Sigma	A5316	IB	ND	human and mouse
14	Normal rat IgG	Abcam	ab18450	control IP	ND	rat
15	Normal mouse IgG	Millipore	12-371	control IP	ND	mouse
16	Normal rabbit IgG	Millipore	12-370	control IP	ND	rabbit

Supplemental Table S3. Antibodies used in this study. IB: Immunoblotting, IP: Immunoprecipitation, IF: Immunofluorescence

Table S4

Source	Gene	Primer sequence (5'- 3')
Human	AGO2_F	ACCCACCCACCGAGTTCGAC
Human	AGO2_R	AGTGCGAAGGCCTGCTTGTC
Human	GAPDH-F	TGTAGTTGAGGTCAATGAAGGG
Human	GAPDH-R	GAGTCCTTCCACGATACCAAAG
Human	AGO2_orf_F	GCACTATCACGTCCTCTGGG
Human	AGO2_orf_R	GGTGTGACACAGCTGGTAGG
Human	KRAS_orf_F	ACACAAAACAGGCTCAGGACT
Human	KRAS_orf_R	AGGCATCATCAACACCCTGT
Human	KRAS_F	TCGACACAGCAGGTCAAGAGGAG
Human	KRAS_R	AGAAAGCCCTCCCCAGTCCTCA
Mouse	MYCN	ACAGAACTGATGCGCTGGAAT
Mouse	MYCN	GGCTGAAGCTTACAGTCCCAA
Mouse	HMGA1_F	CCTCTGGACGGTTGTGTTGT
Mouse	HMGA1_R	TGGGGGAGAGAATACAGGCA
Mouse	HMGA2_F	TGTGCCCTCTGACTTCGTTT
Mouse	HMGA2_R	AGCAAGCCGTCCAAGTACAA
Mouse	KRAS_F	GTTAGCTCCAGTGCCCCAAT
Mouse	KRAS_R	ATTCCCTAGGTCAGCGCAAC
Mouse	SMAD4_F	GGGGAGGGATTTTTCCCTTAAT
Mouse	SMAD4_R	CACCTTGCAGAACAGTGAAGC

Supplemental Table S4. PCR primers used in this study. orf:open reading frame

METHODS SUMMARY

Cell lines, specimen collection

Cell lines, outlined in **Supplemental Table S1**, were purchased from the American Type Culture Collection (ATCC). No further testing for Mycoplasma was performed in the lab. PDX1319 cells were obtained through the Xenograft Core, University of Michigan, directed by Dr. Diane Simeone, University of Michigan, Ann Arbor. Cells were grown in specified media supplemented with serum and antibiotics as per ATCC instructions. Cells were routinely checked for mycoplasma and genotyped to ensure authenticity of cells used.

Coimmunoprecipitation and Tandem Mass Spectrometric analysis

Methods used for immunoprecipitation with RAS/control IgG followed by Tandem Mass Spectrometric analysis and database searching are schematically outlined in **Supplemental Figure S1D**. Complete data of the peptides represented in the RAS co-IP mass spectrometric analysis from the different cell lines are provided in **Supplemental Table S5**. Clustal W analysis was performed using the online program, <http://www.ebi.ac.uk/Tools/services/web/toolform.ebi?tool=clustalo> with peptide sequences obtained from RAS co-IP MS analysis of H358 lung cancer cells.

Immunoprecipitation (IP) and Western blot Analysis

Fresh protein extracts were prepared by lysis of cells in K buffer (10mM Tris HCl, 0.1%, 150mM NaCl, 1% Triton X100 and protease inhibitors). After brief sonication, debris were removed by centrifugation. For IP, 50-400 µg of lysates were pre-cleared with Protein A/G agarose beads (Pierce) for 1 hour and treated overnight at 4°C with 1-10 µg of isotypic control or specific antibody as indicated. The immune complexes were then precipitated with Protein A/G agarose beads, washed with K buffer and resuspended in sample loading buffer. RAS10 monoclonal antibody immunoprecipitates were routinely washed at 500mM NaCl for increased stringency and a final wash was carried out with buffer containing 150mM NaCl prior to SDS-PAGE analysis. When AGO2 antibodies were used for immunoprecipitation, the immunoprecipitates were washed with 300mM NaCl containing K-buffer. RNase/DNase treatments of lysates as well as addition of commercial RNA (obtained from Clontech) were performed prior to pre-clearing of lysates followed by IP. After SDS-PAGE separation, proteins were transferred onto nitrocellulose membranes for immunoblot analysis. For IP using FLAG tagged constructs, FLAG M2 agarose beads (Sigma) were used as per manufacturers' protocol. Antibodies used in the study are detailed in **Table S3**.

Cell Fractionation and Sucrose Density Co-sedimentation analysis Cellular fractions into cytosolic, membrane and nuclear compartments were prepared using Proteoextract Subcellular Proteome Extraction Kit (Millipore), according to manufacturers' instructions. Enrichment of the fractions was validated using antibodies as indicated. Sucrose gradient fractionations were performed as described earlier (Hock et al., 2007). Briefly, cells were lysed in buffer containing 25 mM Tris-HCl (pH 7.4), 150 mM KCl, 0.5% NP-40, 2 mM EDTA, 1 mM NaF, 0.5 mM dithiothreitol and protease inhibitors (Roche) and centrifuged at 10,000g for 10 min at 4°C. For fractionations, gradients from 15% (w/v) to 55% (w/v) sucrose in 150 mM KCl, 25 mM Tris (pH 7.4) and 2 mM EDTA were used. Lysates were separated by centrifugation at 30,000 r.p.m. for 18 h in an SW41 rotor at 4°C. For each lysate 22 fractions of 0.5ml each were collected, 45µl of which was used for immunoblot analysis.

KRAS and AGO2 plasmid constructs

Full length FH-AGO2 and mutant *KRAS*^{G12V} constructs were obtained from Addgene (pIRESneo-FLAG/HA-AGO2 corrected plasmid 10822, PI:Thomas Tuschl; FLAG-AGO2 plasmid 21538: PI: Edward Chan and plasmid 12544 PI: Channing Der). Deletion constructs of AGO2 spanning different domains (indicated in the figures) were subcloned as FLAG-tagged expression plasmids in pDEST40 (Life Technologies) vector backbone. Site directed mutagenesis was performed on AGO2 encoded plasmid 10822 to obtain the constructs described in **Figure 3C**. Site directed mutagenesis was performed on the *KRAS*^{G12V} encoding plasmid to obtain wild type *KRAS4B* and *KRAS*^{G12V/Y64G} constructs in the pBabe-puro vector. All constructs were sequence verified by Sanger sequencing at the University of Michigan Sequencing core.

Cell transfection

NIH3T3 or HEK293T cells were transfected with the indicated plasmid constructs using Fugene HD (Promega) according to standard protocols.

Recombinant KRAS and AGO2 proteins

Human derived KRAS^{WT} and KRAS^{G12V} full length coding regions were cloned as HIS-SUMO tagged proteins in a pET21d plasmid backbone described earlier (Weeks et al., 2007). Site directed mutagenesis was used to introduce the specific mutations described in **Figure 4E-D**. Individual recombinant KRAS proteins were transformed into Rosetta cells for bacterial expression. Cells were resuspended from 1L culture in 40ml of Lysis Buffer (25mM HEPES pH 7.5, 200mM NaCl, A/L, 0.1% bME, 44ul Aprotinin and Leupeptin). Ultra-sonicated for 3 min (6 x 30s, with 30s pause in between) and centrifuged at 17,000rpm in SS34 rotor for 45min to get clear cell lysate. 5 mL Ni-NTA resin was pre-equilibrated (wash) with Lysis Buffer. The cleared cell lysate was then added to the Ni-NTA resin and rotated at 4°C for 1 h followed by centrifugation of Ni resin for 3 min at 1000 x g. The resin was washed 5 times with Ni Wash Buffer 1 (25mM HEPES pH 7.5, 200mM NaCl). Washed Ni-NTA resin was then loaded onto a column and washed using 10 volumes of buffer. Protein was eluted with 25ml total of Ni Elution Buffer 1 (25mM HEPES pH 7.5, 200mM NaCl, 300mM Imidazole), allowed to sit for 10 minutes after the second loading. Quantitation of protein was performed using Nano Drop. SUMO protease in SUMO buffer (25mM HEPES pH 7.5, 150mM NaCl, 1mM DTT) was then added to the eluate, then pour into YM-10 and overnight at 4 C. Protein was then dialysed into 25mM HEPES pH 7.5, 150mM NaCl, 10% Glycerol and stored at -80C before use.

His tagged KRAS^{G12D} (1-166aa) and KRAS^{G12DY64G} (1-166aa) were provided by Gideon Bollag (Plexxikon Inc.). His-tagged AGO2 was cloned in baculoviral vector and purified using Ni-NTA columns.

***In vitro* co-immunoprecipitation**

One hundred nanograms of baculoviral AGO2 or AGO1 proteins (Sino Biologicals) and 50 nanograms of the indicated KRAS protein, were incubated in the above mentioned K-buffer with the addition of 0.2% BSA. After 2 hours of incubation at 4°C, 1µg of IgG (RAS or control) was added and incubated further for 2 hours. 10ul of Protein A/G agarose beads (50% slurry) equilibrated in K buffer were then added to pull down the immune complexes, washed five times at RT and resolved using SDS-PAGE prior to immunoblot analysis.

His-AGO2 pull down assay

Thirty micrograms of his-AGO2 (made in house) protein was incubated with 600ul of Ni-NTA or Cobalt-NTA beads, 50% slurry (Qiagen) resuspended in Ni-NTA buffer (20 mM Tris-HCl (pH.8), 0.1% beta-mercaptoethanol, 150 mM NaCl, 0.5% Triton X-100). Loading performed at 4°C for 1hr. Subsequently the beads were washed using Ni-NTA buffer and incubated with 25 µl of control/His-AGO2 loaded beads with KRAS proteins in Ni-NTA buffer containing 0.2% BSA. Following incubation for 1.5 h at 4 °C and 5 washes were performed at room temperature with rotation for 5 minutes each and centrifugation at 4000 rpm for 2 min. Finally the binding was assessed by immunoblot analysis (using RAS10 and AGO2 11A9 antibodies).

RAS-GTP pull down assay

The RAS-RAF interaction was studied using the RBD agarose beads as per manufacturer's instructions (Millipore). Lysates were prepared upon lysis in MLB (125mM HEPES, pH 7.5, 750mM NaCl, 5% IGEPAL CA-630, 50mM MgCl₂, 5mM EDTA). Lysates were sonicated for 10 seconds, centrifuged to remove debris and cleared lysate was used for binding analysis. 5 microliters of the RAF1-RBD-agarose beads were incubated with the indicated clear lysates for 5 minutes and washed two times in MLB prior to immunoblot analysis. The pull down of RAS by RBD agarose beads indicates the presence of active GTP-bound RAS interacting with RAF1.

Immunofluorescence

Cells were fixed in 4% paraformaldehyde, permeabilized with PBS containing 0.1% triton-x100 or 0.05% saponin, blocked in PBS containing 2% normal goat serum (with or without saponin) and stained with (1:200 dilution) of primary antibody and (1:400 dilution) of secondary antibody diluted in blocking solution. The following primary antibodies were used: rabbit-anti-PD1 (endoplasmic reticulum marker, CST), rabbit-anti-COXIV (mitochondrial marker, CST), rabbit-anti-RCAS1 (golgi marker, CST), rabbit-anti-Rab5/7/11 (endosomal markers, CST), rat-anti-Ago2 (Sigma), rabbit-anti-Ago2 (Millipore) and mouse-anti-RAS (Millipore). The following secondary antibodies from Jackson Immuno-Research were used: goat-anti-rabbit-Alexa488, goat-anti-rat-Cy3 and goat-anti-mouse-Cy5. Imaging was performed as described (Pitchiaya et al., 2012; Pitchiaya et al., 2013) using a cell-TIRF system based on an Olympus IX81 microscope equipped with a 60x 1.49 NA oil-immersion objective (Olympus), as well as 405

nm (Coherent[®], 100 mW at source, ~65 μ W for imaging Alexa-405), 488 nm (Coherent[®], 100 mW at source, ~38 μ W for imaging fluorescein), 532 nm (Coherent[®], 100 mW at source, ~8.5 mW for imaging Cy3) and 640 nm (Coherent[®], 100 mW at source, 13.5 mW for imaging Cy5) solid-state lasers. A quad-band filter cube consisting of a z405/488/532/640rpc dichroic filter (Chroma) and z405/488/532/640m emission filter (Chroma) was used to filter fluorescence of the appropriate fluorophore from incident light. Emission from individual fluorophores was detected sequentially on an EMCCD camera (Andor Ixon). Image processing was performed in Imaris (surface rendering) and ImageJ (background correction) and colocalization analysis was done in Image J (using the Coloc 2 plugin).

shRNA mediated knockdown and cell proliferation assays

H358, H460, MIA PaCa-2 and Panc-1 cells were treated with two independent shRNAs in viral vectors (validated Mission shRNA lentiviral particles, Sigma) targeting *KRAS* (TRCN0000040149, TRCN0000010369, TRCN0000040149) or *AGO2* (TRCN0000007865 and TRCN0000011203). After 5 days, cells were trypsinized and plated in triplicate at 5,000 cells per well in 24-well plates. For NIH3T3 stable lines, cells expressing the indicated plasmids were plated as mentioned earlier. The plates were incubated at 37 °C with 5% CO₂. Cells were counted using Coulter counter at the indicated times.

Colony formation assay

Cells were treated with lentiviral particles expressing *AGO2* shRNA sequences in 6 well dishes. To select stably transfected clones, puromycin at 1 μ g/ml was added to the cells two days after transfection and allowed to grow over 10 days. Medium with selection antibiotic was changed every 2 days. Dishes were then stained using crystal violet, washed with water and photographed.

Focus formation assay

Foci formation assays were performed by transfecting/co-transfecting (the indicated constructs) 150,000 early passage NIH3T3 cells in 6 well dishes using Fugene HD (Promega). After two days, cells were trypsinized and plated onto 150 mm dishes containing 4-5% calf serum. The cells were maintained under low serum conditions and medium was refreshed every two days. After 21 days in culture the plates were stained for foci using crystal violet. Foci were also observed under the microscope to see the altered morphology and were counted manually. Three independent experiments were performed for each condition.

Generation of NIH3T3 stable lines

Early passage NIH3T3 mouse fibroblast cells were plated to 70% confluency and the indicated constructs were transfected using Fugene HD (Promega). Cells transfected with *KRAS*^{G12V}, upon selection with puromycin (1 μ g/ml), showed distinct transformed morphology and continued to proliferate as clusters of cells (unlike naïve NIH3T3 cells). The *KRAS*^{G12V} cells continued to grow in the absence of selection antibiotic and were further transfected with either empty vector (pDEST40) or FLAG-*AGO2* constructs. All the above transfected cells were then selected using G418 (200 μ g/ml).

Site directed mutagenesis was performed to generate Y64G mutation in the *KRAS*G12V plasmid, Addgene 12544, described earlier. NIH3T3 cells were transfected with this construct, selected using puromycin to generate polyclonal population of cells stably expressing *KRAS*^{G12VY64G}.

Generation of NIH3T3 *AGO2*^{-/-} line

AGO2-knockout NIH3T3 cells were generated by CRISPR-Cas9-mediated genome engineering (Ran et al., 2013). Genomic regions in murine *AGO2* between exons 8 and 9, and between exons 11 and 12 were targeted for deletion using primers TCCTTGTTACCCGATCCTGG and AGAGACTATCTGCAACTATGG, respectively (PAM motif underlined). PCR products were cloned into the BbsI site of pX458 (pSpCas9(BB)-2A-GFP; obtained from the laboratory of Feng Zhang via Addgene (Cambridge, MA; plasmid 48138)) according to the cloning protocol provided by the Zhang lab (<http://www.genome-engineering.org>). Cells were transfected with the vectors using Lipofectamine 3000 (Life Technologies) according to the manufacturer's instructions. 48 hours post-transfection, GFP-positive cells were FACS sorted as a single cell into 96-well plate. After culturing for 3 weeks, cells are distributed into two 24 well plates followed by PCR-based genotyping using primers mentioned above. A clone showing deletion of the targeted region in *AGO2* was used for further analysis. Single-cell sorted cells obtained after

transfection of the empty pSpCas9(BB)-2A-GFP construct was used as a negative control. NIH3T3 AGO2^{-/-} cells were also transfected with the KRASG12V plasmid construct to generate stable cell lines after puromycin selection.

Xenograft Models

Five week-old male C.B17/SCID mice were procured from a breeding colony at the University of Michigan. Mice were anesthetized using a cocktail of xylazine (80 mg/kg, intraperitoneal) and ketamine (10 mg/kg, intraperitoneal) for chemical restraint. NIH3T3 cells stably expressing AGO2, KRAS^{WT}, KRAS^{G12V}+vector or KRAS^{G12V}+AGO2 (0.5 or 1 million cells for each implantation site) were resuspended in 100 μ L of 1 \times PBS with 20% Matrigel (BD Biosciences) and were implanted subcutaneously into flank region on both sides. Eight mice were included in each experimental group. Tumor growth was recorded every two days by using digital calipers, and tumor volumes were calculated using the formula ($\pi/6$) (L \times W²), where L = length of tumor and W = width. For the Mia PaCa-2 xenograft model, cells were first treated with either scrambled or AGO2 shRNA overnight. After 2 days of puromycin selection the cells in each group were injected in 8 mice and the progression of tumor growth was monitored over time. To study oncogenic potential of NIH3T3 KRAS^{G12VY64G} and NIH3T3 AGO2^{-/-} cells *in vivo*, subcutaneous implantation of cells on both flanks of mice were performed as before (n=5 mice).

Four to five week old female SCID mice were used for all xenograft studies. Based on power calculation (<http://www.biomath.info/power/index.htm>), we determined that less than 6 mice per group are sufficient to detect significant differences in tumor volumes between two groups. All mouse experiments were done in a blinded fashion with mice being randomly selected for experiments. The person performing the measurements was blinded to the treatment groups. No animals were excluded in any of the xenograft experiments. All experimental procedures involving mice were approved by the University Committee on Use and Care of Animals at the University of Michigan and conform to their relevant regulatory standards.

Quantitative microRNA and mRNA RT-PCR

For the quantitation of microRNA levels in the NIH3T3 cells transfected with indicated constructs (from both the transient foci assays and stable lines), total RNA was prepared using the miRNeasy kit (Qiagen). MicroRNA RT-qPCR was performed according to the manufacturer's instructions (Applied Biosystems). U6 RNA was used as the endogenous control since its Ct values remained consistent. The vector transfected cells were used as reference. For quantitation of mRNA transcripts, RNA was extracted from the indicated samples and cDNAs were synthesized using SuperScript III System according to the manufacturer's instructions (Invitrogen). Quantitative RT-PCR was conducted using primers detailed in **Table S4** with SYBR Green Master Mix (Applied Biosystems) on the StepOne Real-Time PCR System (Applied Biosystems). Relative mRNA levels of the transcripts were normalized to the expression of the housekeeping gene *GAPDH* and vector transfected cells were used as reference.

iSHIRLoC analyses

RNA oligonucleotides were purchased from Exiqon and IDT, respectively. RNA oligos were obtained with a 5' phosphate and for the let-7-a1 guide strand, with a 3' Cy5 modification. All oligos were HPLC purified by the appropriate vendor. Oligonucleotide sequences are as follows,

let-7-a1 guide: P-UGA GGU AGU AGG UUG UAU AGU U-Cy5

let-7-a1-passenger: P-CUA UAC AAU CUA CUG UCU UUC C

RNA oligos were heat-annealed in a 1:1 ratio in 1x PBS, resulting in duplex RNAs, and were frozen for further use. Cells were cultured in DMEM (GIBCO) supplemented with 10% (v/v) calf serum (CS, Colorado serum) and 1x penicillin-streptomycin (GIBCO) at 37 °C. Cells (1 - 1.25 \times 10⁵) were seeded onto delta-T dishes (Bioptechs) 4 days prior to microinjection, such that they were ~80% confluent at the time of microinjection. Regular medium was replaced with a minimal medium (HBS), without serum and vitamins, but containing 20 mM HEPES-KOH pH 7.4, 135 mM NaCl, 5 mM KCl, 1 mM MgCl₂, 1.8 mM CaCl₂ and 5.6 mM glucose immediately before microinjection. After microinjection, cells were incubated in phenol red-free DMEM containing 2% (v/v) CS in the presence of a 5% CO₂ atmosphere at 37 °C for the indicated amounts of time prior to imaging.

Microinjection was performed with samples containing 1 μ M Cy5 labeled let-7-a1 duplexes and 0.05% (w/v) 10 kDa fluorescein dextran (Invitrogen) in PBS. Imaging was performed as described (Pitchiaya et al., 2012; Pitchiaya et al., 2013) using a cell-TIRF system based on an Olympus IX81 microscope equipped with a 60x 1.49 NA oil-immersion objective (Olympus), as well as 488 nm (Coherent[®], 100 mW at source, ~38 μ W for imaging fluorescein) and 640 nm (Coherent[®], 100 mW at source, 13.5 mW for imaging Cy5) solid-state lasers. A quad-band filter cube consisting of a z405/488/561/640rpc dichroic filter (Chroma) and z405/488/561/640m emission filter (Chroma) was used to filter fluorescence of the appropriate fluorophore from incident light. Emission from

individual fluorophores was detected sequentially on an EMCCD camera (Andor Ixon). Particle tracking analysis was performed by using tracks that spanned at least four video frames.

Extract preparation and in vitro miRNA unwinding assay

Cell extracts were prepared as described (Kwak et al, Nat. Struct. Mol. Boil. 2012 and Rakotondrafara et al, Nature protocols, 2011), with minor modifications. Briefly, cells grown in 150 cm² flasks (4x per cell line) were trypsinized, diluted with equal volume of FBS containing media and collected by centrifugation at 1500g for 5 min at 4°C. Cells were washed 2 times with cold PBS and resuspended in hypotonic lysis buffer (10mM HEPES-KOH, pH 7.5, 10mM potassium acetate, 0.5 mM magnesium acetate, 0.1 % Igepal, 0.1% Tween-20). Cells were incubated at 4°C for 30 min and the suspension was passed 5-10 x through a 27.5-G needle to promote lysis. The cell extracts were then cleared by centrifuging at 20,000g for 10 min at 4°C and the supernatant were flash frozen and stored at -80°C until use. All buffers contained 1x EDTA-free protease inhibitor cocktail. We typically obtained 15-20 mg/mL protein concentration in the extract. Unwinding assays were performed as described (Nykanen et al, Cell, 2001) with some minor modifications. 10 uL reactions containing 250 fmol double stranded let-7 miRNA (Cy5 labeled at the 3' end of the guide strand and Cy3 labeled in the 3' end of the passenger strand), 75 µg cell extracts, 30 mM HEPES, pH 7.4, 100 mM potassium acetate, 2 mM magnesium acetate, 5 mM DTT, 0.33x protease inhibitor cocktail (Roche), 25 mM creatine phosphate, 1 mM ATP, 0.05 U/uL rRNAsin (Promega) and 0.5 U/uL creatine kinase, were incubated for 10 min at 4°C and 25°C. Then, 2500 fmol of unlabeled guide strand was added to the reaction along with proteinase K (2mg/mL) and the reaction was incubated at 25°C for an additional 10mins. Samples were rapidly transferred to ice, mixed with 2.5 uL of 5x gel loading buffer (50mM Tris.HCl, 0.5% SDS, 0.1% NP40, 50% glycerol) loaded onto 20% TBE gels (10cm x 10cm) and electrophoresed at 200 V for 2.5 h at 4°C. Gels were then scanned using a Typhoon scanner (GE) and bands were quantified using Image J.

Pathscan Intracellular signaling array analysis

Pathscan intracellular signaling arrays were purchased from Cell Signaling. Indicated cells from the overexpression model or after knockdown were serum starved overnight and 40-80 µg of lysates generated from these were applied to the arrays. Arrays were processed according to the manufacturer's instructions and developed using chemiluminescent substrates. For analysis the ImageJ software was used and control spots indicated in **Figure S5C** were used to normalize the data. The quantitative bar charts shown in the study are for those signaling molecules that show intensity levels of greater than 50 for each of the duplicate spots in a given treatment such as overexpression or knockdown.

microRNA Sequencing

microRNA libraries for sequencing were prepared using the "Illumina® TruSeq® Small RNA Sample Preparation" protocol following the manufacturer's instructions. Briefly, one microgram of total RNA from NIH3T3 foci expressing *KRAS*^{G12V}+vector or *KRAS*^{G12V}+*AGO2* was sequentially subjected to 3' and 5' RNA adaptor ligations. The adaptor ligated RNA was converted to cDNA using Superscript II reverse transcriptase and RNA RT primer. The samples are then subjected to 11 cycles of PCR amplification and in the process barcoded. The PCR products were ethanol precipitated and resolved using a 6% TBE PAGE gel, electrophoresed at 145V for 60 minutes. The PCR products observed between 145 and 160 base pairs were excised and passed through a gel breaker tube at 20,000g for 2 minutes. The DNA was eluted from the gel pieces overnight, ethanol precipitated and its size and concentration analyzed by Bio-Analyzer. The barcoded microRNA libraries were sequenced using the Illumina MiSeq sequencing machine.